

Nonlinear effect of uniaxial pressure on superconductivity in CeCoIn₅

S. D. Johnson and R. J. Zieve

Physics Department, University of California, Davis, Davis, California 95616, USA

J. C. Cooley

Los Alamos National Laboratory, Los Alamos, New Mexico 87545, USA

(Received 16 October 2010; revised manuscript received 22 February 2011; published 14 April 2011)

We study single-crystal CeCoIn₅ with uniaxial pressure up to 3.97 kbar applied along the *c* axis. We find a nonlinear dependence of the superconducting transition temperature T_c on pressure, with a maximum close to 2 kbar. The transition also broadens significantly as pressure increases. We discuss the temperature dependence in terms of the general trend that T_c decreases in anisotropic heavy-fermion compounds as they move toward three-dimensional behavior.

DOI: [10.1103/PhysRevB.83.144510](https://doi.org/10.1103/PhysRevB.83.144510)

PACS number(s): 71.27.+a, 74.62.Fj, 74.70.Tx

I. INTRODUCTION

The past three decades have seen the discovery of several new groups of superconductors that do not conform to the previous understanding of superconductivity: the cuprates,¹ heavy fermions,² organics,³ and the very recent pnictide superconductors.⁴ Although behavior varies substantially among these materials, in many cases, even for closely related compounds, similarities include deviations from Fermi liquid behavior^{5–8} and the appearance of superconductivity near the quantum critical point where a magnetic transition is suppressed to zero temperature.^{9–11} From these observations a general picture is emerging of superconductivity with Cooper pairs bound by magnetic fluctuations. The magnetic interaction favors the *d*-wave pairing symmetry which has been established in the cuprates¹² and indicated elsewhere.^{13–16} Low dimensionality also facilitates superconductivity,^{17,18} since the pairing interaction falls off less quickly in lower dimensions.

The 115 superconductors, CeMIn₅ [M = Co (Ref. 19), Rh (Ref. 20), Ir (Ref. 21)] and the isostructural PuMGa₅ [M = Co (Ref. 22), Rh (Ref. 23)] family, are useful materials for testing effects of dimensionality. Both families are heavy-fermion superconductors that also exhibit antiferromagnetism, sometimes in concert with superconductivity. They are clean, relatively easy to grow, and close to a quantum critical point at ambient pressure. The crystal structure is tetragonal, with alternating layers of CeIn₃ and MIn₂, resulting in anisotropic superconductivity. For the 115 materials, including several alloys where M is a mixture of two elements, the superconducting transition temperature T_c increases linearly with c/a within a family,²⁴ with the same logarithmic derivative $\frac{d(\ln T_c)}{d(c/a)}$ for both the Ce and Pu families.²⁵ In several cases uniaxial pressure adheres to this trend. By pushing the planes together, *c*-axis pressure should decrease T_c . On the other hand, *a*-axis pressure increases the plane separation and should increase T_c . For CeIrIn₅, uniaxial pressure has exactly these effects, with measurements made both directly²⁶ and by extracting the zero-pressure dT_c/dP from thermal expansion data.²⁷ However, for CeCoIn₅, thermal expansion measurements yield positive $\frac{dT_c}{dP}|_{P=0}$ for *c*-axis pressure as well as for *a*-axis pressure.²⁷ Here we apply uniaxial pressure along the *c* axis of CeCoIn₅ to investigate this apparent exception to the pattern that higher dimensionality corresponds to lower T_c .

II. MATERIALS AND METHODS

Single-crystal samples were grown in aluminum crucibles containing stoichiometric amounts of Ce and Co with an excess of In. The crucibles were sealed in quartz tubes, heated to 1150°C, and slow cooled to 450°C. Excess flux was removed by centrifuging. CeCoIn₅ grows in thin platelets perpendicular to the crystal *c* axis. To prepare samples for pressure measurements, we removed excess In and polished the faces to be smooth and free of chips or defects. The polishing also ensures that the faces used for pressure application are parallel to each other. We confirmed the sample orientation by x-ray diffraction, both before and after polishing.

We applied uniaxial pressure using a bellows setup activated with helium gas from room temperature. The pressure cell is permanently mounted on an Oxford Instruments dilution refrigerator. A piezosensor monitors the force in the pressure column (see Ref. 26 for pressure setup schematic). With this setup, we can reach a maximum pressure of about 10 kbar, depending on the cross-sectional area of the sample, and we can change pressure in controlled steps smaller than 0.1 kbar.

From the mass and thickness of the sample, we computed its cross-sectional area, which we then used to calculate the pressure on the sample. The data shown here are from a sample with mass 2.43 mg and area 1.54×10^{-6} m². Measurements of a second sample of mass 0.57 mg and area 3.63×10^{-7} m² agreed qualitatively, although the smaller sample size reduced the quality of the data.

A screw at one end of the pressure column controls its overall length. We finger-tightened this screw while watching the pressure monitor, applying a pressure of about 0.05 kbar to the sample at room temperature. This ensures that the sample remains in place while we load the cryostat into its dewar and cool from room temperature. Thermal contraction during cooling may alter the initial pressure; in previous work the initial pressure appeared on the order of 0.3 kbar at low temperatures.²⁶ The values for applied pressure used in this paper do not include any offset for this initial pressure, but our initial transition temperature measurements agree to better than 3 mK with measurements taken outside of the pressure cell, suggesting a pressure offset of less than 0.2 kbar. Once the cryostat was below 4 K, we filled the bellows with liquid helium. We then increased pressure in steps of about 0.5 kbar. The maximum pressure used here is 3.97 kbar.

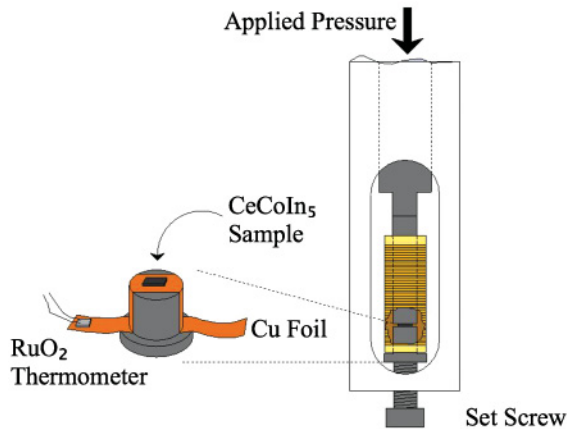


FIG. 1. (Color online) A balanced ac-susceptibility coil is placed around the pressure shafts. The sample is between the two shafts of the pressure column, centered in one of the pickup coils.

In the present measurements, the effect of pressure was reversible. The data shown here come from three pressure sweeps on the sample, the first reaching a maximum pressure of 2.60 kbar, the second 3.97 kbar, and the third 2.86 kbar. After completing the measurements, we confirmed by x-ray diffraction that the sample retained its original crystal structure.

We detected the transition to the superconducting state with a balanced ac-susceptibility coil that accommodates the pressure shafts and the sample, as shown in Fig. 1. The outer primary coil is 0.9 in. long with inner diameter 0.35 in. It contains approximately 600 turns of 0.006-in.-diam Cu wire and with our usual settings generates a field of about 0.3 gauss parallel to the pressure shafts. The inner secondary coils are wound on a cylinder of diameter of 0.16 in. and contain 200 turns each of 0.002-in.-diam Cu wire. The inner coils are separated by 0.325 in., so there is minimal field interaction between coils. We monitored the signal from the inner coils using a Linear Research LR-700 resistance bridge. We positioned the sample so that its entire volume is contained within the bottom coil of the secondary.

To ensure that the sample is in thermal contact with the mixing chamber, we varnish Cu foil to the pressure shafts on either side of the sample, with the other end of each foil varnished to the mixing chamber. Even with the Cu foil heat sink, the large thermal mass of the pressure setup results in a temperature lag between the sample and the mixing chamber during temperature scans. We monitored the sample temperature directly using a RuO₂ thermometer mounted on the copper foil within 0.5 in. of the sample.

III. RESULTS AND DISCUSSION

Figure 2 shows the superconducting transition for several pressures. The substantial broadening of the transition with pressure ensures that the midpoint moves down in temperature with increasing pressure. However, as shown in the inset, the onset behaves differently, initially moving to *higher* temperature as pressure increases. Here we identify the onset as the highest temperature at which the susceptibility χ deviates from its constant normal-state value χ_n . We plot the onset

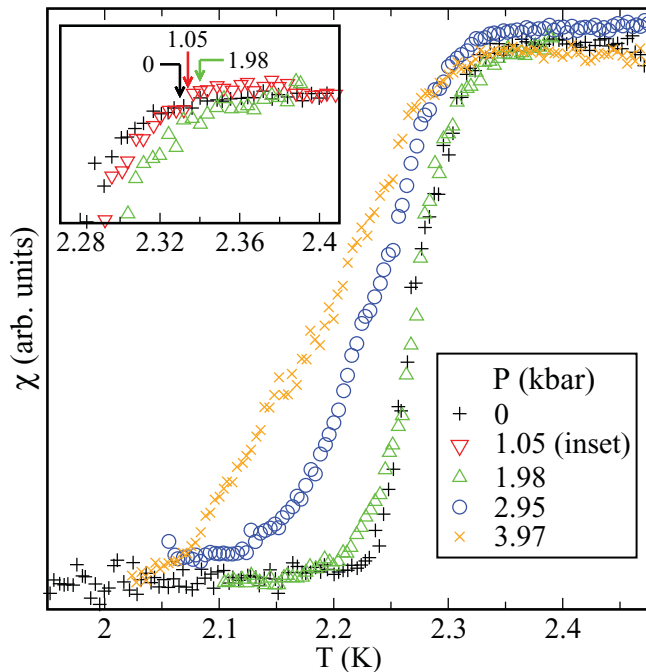


FIG. 2. (Color online) Representative data showing the effect of *c*-axis uniaxial pressure. The transition width ΔT_c is strongly pressure dependent, whereas the onset temperature T_c is not. The inset expands the region near T_c to reveal a slight increase in T_c with pressure. Arrows indicate the onset T_c for each curve.

temperatures T_c in Fig. 3. The parabola, with a maximum near 2 kbar, is a least-squares fit.

The nonmonotonic $T_c(P)$ makes it particularly important to consider the meaning of the transition width. The width ΔT_c , defined as the difference between onset of superconductivity and the leveling off of χ at the low end of the transition, increases from 112 mK at zero pressure to 270 mK at 3.97 kbar,

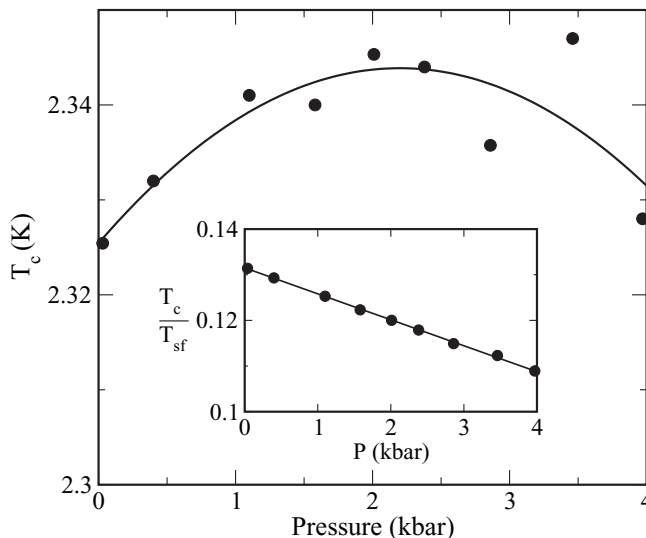


FIG. 3. Onset temperature for superconductivity as a function of pressure. The points are averages over measurements at similar applied pressures P_{app} , and the curve is a quadratic fit. Inset: T_c/T_{sf} vs pressure, with a linear fit shown. As described in the text, T_{sf} values are adapted from hydrostatic pressure measurements.

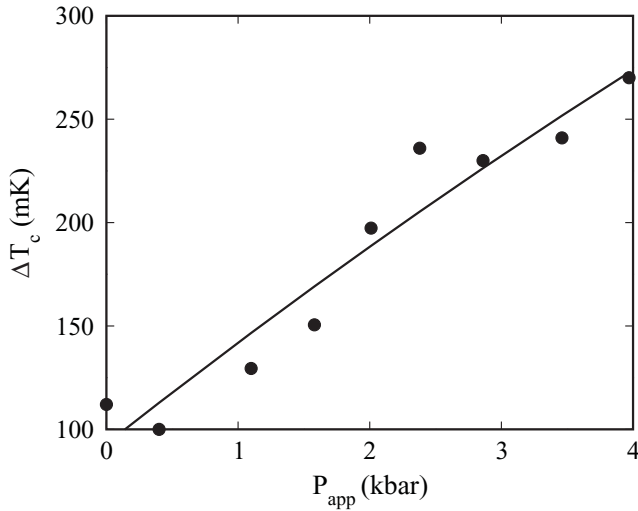


FIG. 4. Superconducting transition width vs applied pressure. Solid line is the best linear fit to the data.

as shown in Fig. 4. One possible source for the broadening is nonuniformity in the applied pressure. The pressure dependence of T_c would then lead to different transition temperatures in different parts of the sample. Nonuniform pressure could arise from a variety of effects, such as defects in the sample, variation in its cross-sectional area, indium inclusions, surface irregularities, a tilt in the pressure column, or an intrinsic inhomogeneity in the pressure distribution within the sample.

We have estimated the pressure inhomogeneity needed to produce the observed broadening, using various assumptions for the distribution of c -axis pressure within the sample. We find that, to account for the entire increase in transition width, the pressure would have to vary by more than a factor of 2 across the sample. This is a consequence of the scant change in the onset temperature of the transition. Either the transition has little pressure dependence, in which case variations of pressure would not broaden it, or a portion of the sample remains at very low pressure even when the nominal applied pressure is large. Although a nonconstant sample cross section or an angle of the pressure spacers could cause inhomogeneity of a few percent, a 100% variation is far too extreme.

The pressure could also vary in direction within the sample, creating stress with an a -axis component. However, as noted above, both thermal expansion measurements²⁷ and the expected influence of dimensionality suggest that a -axis pressure would increase T_c , which would not explain the broadening of the transition to lower temperatures that we observe. We conclude that, if the transition width truly signifies pressure variation, it must indicate a broad distribution of pressure within the sample from an intrinsic mechanism.

Interestingly, in resistivity measurements on CeCoIn₅ under hydrostatic pressure the transition width has a minimum near $P^* = 16$ kbar, the pressure which maximizes T_c .²⁸ The transition width in specific heat exhibits a similar crossover behavior, remaining nearly constant at low pressures but increasing substantially once pressure exceeds 16 kbar.²⁹ The agreement between the different types of measurement is evidence that the width has an intrinsic component. Here

our susceptibility measurements show a substantial increase in transition width from the lowest pressures. If uniaxial c -axis pressure shifts CeCoIn₅ away from the P^* reached with hydrostatic pressure, our observed broadening could plausibly be a tuning effect related to the width changes observed with other techniques.

In the following discussion, we bypass concerns about the origin of the transition width by focusing on the onset temperature. The small initial slope of the T_c curve is consistent with a nearby maximum. Fits to our data suggest $\frac{dT_c}{dP}|_{P=0} = 17$ mK/kbar. The value derived from thermal expansion measurements²⁷ is even lower, 7.5 mK/kbar. This pressure dependence is substantially less than that of CeIrIn₅, where direct c -axis pressure measurements give $\frac{dT_c}{dP}|_{P=0} = -66$ mK/kbar²⁶ and thermal expansion suggests $\frac{dT_c}{dP}|_{P=0} = -89$ mK/kbar.²⁷ The pressure effect is also smaller than for a -axis pressure in CeCoIn₅, where thermal expansion suggests that T_c increases 29 mK/kbar.²⁷ One natural explanation is that CeCoIn₅ at ambient pressure is near an extremum of $\frac{dT_c}{dP}$, particularly for c -axis pressure.

Nonmonotonic behavior is less common with uniaxial pressure than with its hydrostatic counterpart. Partly this is because the maximum pressure is generally much smaller in the uniaxial case, due to sample breakage or to the limits of the pressure apparatus. In addition, a given hydrostatic pressure may affect an isotropic sample in a similar way as three times as much uniaxial pressure, a consequence of applying the pressure simultaneously along all three perpendicular axes. Together these considerations mean that a typical uniaxial pressure measurement tunes a sample over a narrow regime compared to standard hydrostatic techniques.

Hydrostatic pressure measurements on CeCoIn₅ (Ref. 28) find a maximum T_c near 16 kbar. Without anisotropic effects, one might expect an equivalent uniaxial pressure to be 48 kbar, since hydrostatic pressure involves stress applied along all three axes simultaneously. In fact, we find the maximum T_c at a drastically lower pressure near 2 kbar.

The maximum in T_c requires competing factors that tend to raise or lower T_c with applied pressure. The former is the hybridization of neighboring atomic orbitals, which increases as pressure reduces the atomic spacing. Using a tight-binding approximation,^{30–32} we estimate the fractional change in the hybridization between the Ce f electrons and the In p electrons as 0.0665% per kilobar of c -axis pressure. An analogous calculation for CeIrIn₅ gives 0.0653% change per kilobar. The similarity of these values implies that the main difference between the materials lies elsewhere.

The other key factor is sample anisotropy, which decreases with c -axis pressure. This is consistent with our maximum T_c occurring at a much lower pressure than in hydrostatic pressure measurements, since hydrostatic pressure has a more uniform effect on the sample. Calculations also predict that lower anisotropy should decrease superconducting transition temperatures.¹⁸

The calculations track T_c/T_{sf} , where T_{sf} is the spin-fluctuation temperature that appears to set the energy scale in magnetically mediated superconductors. In principle T_{sf} is related to the normal-phase susceptibility just above T_c . However, that susceptibility is quite small and changes only

a few percent per kilobar. All told, the changes in χ_n are about five orders of magnitude smaller than the size of the superconducting transition. Our signal has comparable shifts from other factors, possibly including small changes in sample shape and position with applied pressure. The lack of a measurement of T_{sf} limits the comparison possible with Ref. 18. As a rough illustration of how the behavior of T_{sf} dominates that of T_c , we refer to data under hydrostatic pressure.³³ There T_{sf} , which is assumed proportional to the temperature T_M of the resistance maximum, increases about 6% per kilobar. We ignore anisotropy in the spin fluctuations and reduce the change in T_{sf} to 2% per kilobar to adjust between hydrostatic and uniaxial pressure. With our measured superconducting transition temperatures, we then plot T_c/T_{sf} as a function of applied c -axis pressure, shown in the inset to Fig. 3. The pressure dependence of T_{sf} dominates, changing the low-pressure maximum to a near-linear monotonic decrease. Although the actual dependence of T_{sf} on c -axis pressure may differ from this estimate, for any increase of roughly the same size T_{sf} mainly determines the behavior of T_c/T_{sf} .

That T_{sf} increases with c -axis pressure is consistent with recent experiments on CeIn₃/LaIn₃ heterostructures.³⁴ As the thickness of the CeIn₃ layers decreases, the effective mass increases, an effect attributed to the changing dimensionality. Our c -axis pressure tends to increase dimensionality, which corresponds to a decreasing effective mass and increasing T_{sf} .

IV. CONCLUSION

We present ac-susceptibility measurements on a single-crystal sample of CeCoIn₅ under direct uniaxial pressure up to 3.97 kbar, along the c axis. We find a weak, nonlinear dependence of T_c on pressure. After an initial increase to a maximum near 2 kbar, T_c then decreases. The decrease agrees qualitatively with the behavior expected from decreasing the anisotropy parameter c/a . We also find an increase in transition width as pressure increases that is much larger than would be expected from nonuniformity in pressure and may be connected to our tuning through the superconducting phase.

-
- ¹J. G. Bednorz and K. A. Müller, *Z. Phys. B* **64**, 189 (1986).
²F. Steglich, J. Aarts, C. D. Bredl, W. Lieke, D. Meschede, W. Franz, and H. Schäfer, *Phys. Rev. Lett.* **43**, 1892 (1979).
³D. Jérôme, A. Mazaud, M. Ribault, and K. Bechgaard, *J. Phys. Lett.* **41**, 95 (1980).
⁴Y. Kamihara, H. Hiramatsu, M. Hirano, R. Kawamura, H. Yanagi, T. Kamiya, and H. Hosono, *J. Am. Chem. Soc.* **128**, 10012 (2006).
⁵C. M. Varma, P. B. Littlewood, S. Schmitt-Rink, E. Abrahams, and A. E. Ruckenstein, *Phys. Rev. Lett.* **63**, 1996 (1989); **64**, 497 (1990).
⁶J. Moser, M. Gabay, P. Auban-Senzier, D. Jérôme, K. Bechgaard, and J. M. Fabre, *Eur. Phys. J. B* **1**, 39 (1998).
⁷G. R. Stewart, *Rev. Mod. Phys.* **73**, 797 (2001); **78**, 743 (2006).
⁸W. Wu, A. McCollam, I. Swainson, P. M. C. Rourke, D. G. Rancourt, and S. R. Julian, *Europhys. Lett.* **85**, 17009 (2009).
⁹N. D. Mathur, F. M. Grosche, S. R. Julian, I. R. Walker, D. M. Freye, R. K. W. Haselwimmer, and G. G. Lonzarich, *Nature (London)* **394**, 39 (1998).
¹⁰H. Kotegawa, H. Sugawara, and H. Tou, *J. Phys. Soc. Jpn.* **78**, 013709 (2009).
¹¹L. Taillefer, *Annu. Rev. Cond. Matt. Phys.* **1**, 51 (2010).
¹²C. C. Tsuei and J. R. Kirtley, *Rev. Mod. Phys.* **72**, 969 (2000).
¹³H. Tou, Y. Kitaoka, K. Asayama, C. Geibel, C. Schank, and F. Steglich, *J. Phys. Soc. Jpn.* **64**, 725 (1995).
¹⁴O. Stockert, J. Arndt, A. Schneidewind, H. Schneider, H. S. Jeevan, C. Geibel, F. Steglich, and M. Loewenhaupt, *Physica B* **403**, 973 (2008).
¹⁵Y. Kasahara, T. Iwasawa, Y. Shimizu, H. Shishido, T. Shibauchi, I. Vekhter, and Y. Matsuda, *Phys. Rev. Lett.* **100**, 207003 (2008).
¹⁶K. Ichimura, K. Nomura, and A. Kawamoto, *Jpn. J. Appl. Phys.* **45**, 2264 (2006).
¹⁷P. Monthoux and G. G. Lonzarich, *Phys. Rev. B* **63**, 054529 (2001).
¹⁸P. Monthoux and G. G. Lonzarich, *Phys. Rev. B* **66**, 224504 (2002).
¹⁹C. Petrovic, P. G. Pagliuso, M. F. Hundley, R. Movshovich, J. L. Sarrao, J. D. Thompson, Z. Fisk, and P. Monthoux, *J. Phys. Condens. Matter* **13**, L337 (2001).
²⁰H. Hegger, C. Petrovic, E. G. Moshopoulou, M. F. Hundley, J. L. Sarrao, Z. Fisk, and J. D. Thompson, *Phys. Rev. Lett.* **84**, 4986 (2000).
²¹C. Petrovic, R. Movshovich, M. Jaime, P. G. Pagliuso, M. F. Hundley, J. L. Sarrao, Z. Fisk, and J. D. Thompson, *Europhys. Lett.* **53**, 354 (2001).
²²J. L. Sarrao, L. A. Morales, J. D. Thompson, B. L. Scott, G. R. Stewart, F. Wastin, J. Rebizant, P. Boulet, E. Colineau, and G. H. Lander, *Nature (London)* **420**, 297 (2002).
²³F. Wastin, P. Boulet, J. Rebizant, E. Colineau, and G. H. Lander, *J. Phys. Condens. Matter* **15**, S2279 (2003).
²⁴P. G. Pagliuso, R. Movshovich, A. D. Bianchi, M. Nicklas, N. O. Moreno, J. D. Thompson, M. F. Hundley, J. L. Sarrao, and Z. Fisk, *Physica B* **312–313**, 129 (2002).
²⁵J. D. Thompson, J. L. Sarrao, and F. Wastin, *Chin. J. Phys.* **43**, 499 (2005).
²⁶O. M. Dix, A. G. Swartz, R. J. Zieve, J. Cooley, T. R. Sayles, and M. B. Maple, *Phys. Rev. Lett.* **102**, 197001 (2009).
²⁷N. Oeschler, P. Gegenwart, M. Lang, R. Movshovich, J. L. Sarrao, J. D. Thompson, and F. Steglich, *Phys. Rev. Lett.* **91**, 076402 (2003).
²⁸V. A. Sidorov, M. Nicklas, P. G. Pagliuso, J. L. Sarrao, Y. Bang, A. V. Balatsky, and J. D. Thompson, *Phys. Rev. Lett.* **89**, 157004 (2002).
²⁹G. Knebel, M.-A. Measson, B. Salce, D. Aoki, D. Braithwaite, J. P. Brison, and J. Flouquet, *J. Phys. Condens. Matter* **16**, 8905 (2004).
³⁰W. A. Harrison, *Elementary Electronic Structure* (World Scientific, Singapore, 1999).
³¹J. M. Wills and W. A. Harrison, *Phys. Rev. B* **28**, 4363 (1983).
³²R. S. Kumar, A. L. Cornelius, and J. L. Sarrao, *Phys. Rev. B* **70**, 214526 (2004).
³³M. Nicklas, R. Borth, E. Lengyel, P. G. Pagliuso, J. L. Sarrao, V. A. Sidorov, G. Sparn, F. Steglich, and J. D. Thompson, *J. Phys. Condens. Matter* **13**, L905 (2001).
³⁴H. Shishido, T. Shibauchi, K. Yasu, T. Kato, H. Kontani, T. Terashima, and Y. Matsuda, *Science* **327**, 980 (2010).